Volume 10, Issue 1, June 2023 ISSN 2542-2545

The HIMALAYAN PHYSICS

A peer-reviewed Journal of Physics

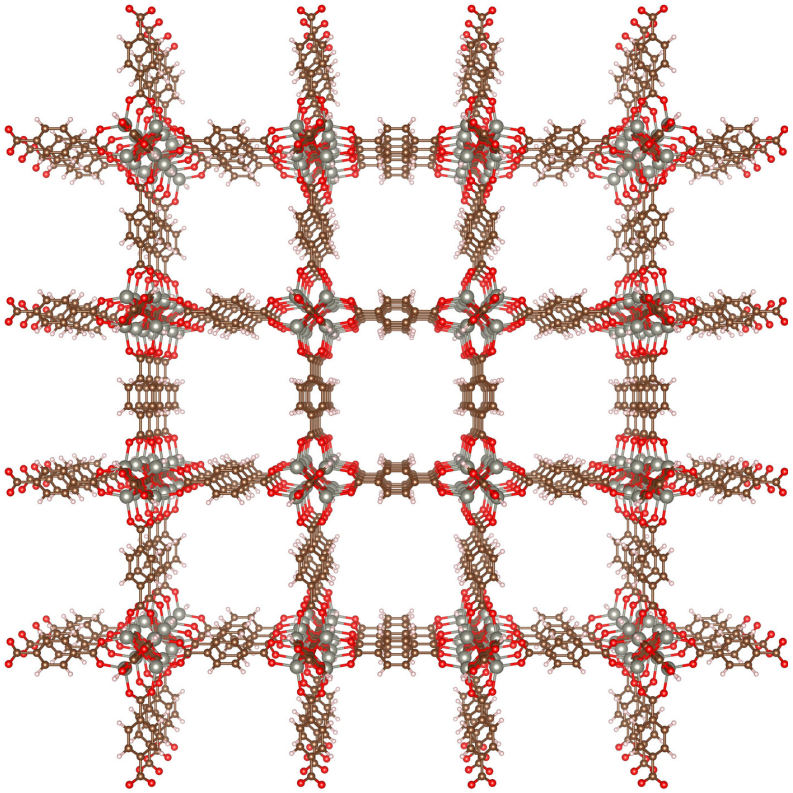

Department of Physics, Prithvi Narayan Campus, Pokhara
Nepal Physical Society, Gandaki Chapter, Pokhara

Publisher

Department of Physics, Prithvinarayan Campus, Pokhara
Nepal Physical Society, Gandaki Chapter, Pokhara

The Himalayan Physics

Volume 10, Issue 1, June 2023

ISSN 2542-2545

The Himalayan Physics (HimPhys) is an open access peer-reviewed journal that publishes quality articles which make innovative contributions in all areas of Physics. HimPhys is published annually by Nepal Physical Society (Gandaki Chapter), and Department of Physics, Prithvi Narayan Campus, Pokhara. The goal of this journal is to bring together researchers and practitioners from academia in Nepal and abroad to focus on advanced techniques and explore new avenues in all areas of physical sciences and establishing new collaborations with physics community in Nepal.

Chief Editor

Aabiskar Bhusal

Cover: Ball-and-stick model of MOF-5. © Roshani Sharma. Printed with permission.

Volume 10, Issue 1, June 2023 ISSN 2542-2545

The HIMALAYAN PHYSICS

A peer-reviewed Journal of Physics

Publisher

Department of Physics, Prithvi Narayan Campus, Pokhara
Nepal Physical Society, Gandaki Chapter, Pokhara

Nepal Physical Society

Gandaki Chapter

Pokhara, Nepal

Himalayan Physics Vol-10(1) (2023)

TABLE OF CONTENTS

****

Him. Phys. **10(1)** 40-50, (2023)

Himalayan Physics

Dust properties around NGC 7023 nebula in interstellar medium using IRIS, AKARI, and WISE survery

Research Article

Anil Subedi[1], Ashok Chaudhary[2], Keshab Chaudhary[2], Kushal Khatiwada[1], Ramchandra Kandel[1], Shiv Narayan Yadav[3], Devendra Raj Upadhyay[1], Ajay Kumar Jha[2]*

1 Department of Physics, Amrit Campus, Tribhuvan University, Kathmandu, Nepal

2 Central Department of Physics, Tribhuvan University, Kathmandu, Nepal

3 Patan Multiple Campus, Patan, Tribhuvan University, Nepal

Abstract: We have studied the physical properties of dust around the nebula NGC 7023. The physical properties have been studied at 60 μm and 100 μm in the IRIS survey, 90 μm and 140 μm in the AKARI survey, and 12 μm and 22 μm in the WISE survey at the right ascension (R.A.) (J2000) = $21^h01^m35.60^s$, declination (J2000) = $+\ 68^o10^m10.0^s$. The nebula is found at a distance of 335.82 pc from us. We found the dust color temperature is in the range between 36.19 K $\pm$ 0.03 K to 24.49 K $\pm$ 0.03 K with an average dust color temperature of 28.24 K $\pm$ 0.03 K in IRIS survey and a range between 38.80 K $\pm$ 0.25 K to 21.00 K $\pm$ 0.25 K with an average dust color temperature 26.39 K $\pm$ 0.25 K in AKARI survey. Similarly, in WISE, the dust color temperature was found in the range between 130.92 K $\pm$ 0.01 K to 88.71 K $\pm$ 0.01 K with an average of 104.76 K $\pm$ 0.25 K. The temperature in WISE is higher than that of the IRIS and AKARI survey. We have also calculated the dust mass, whose average value was found to be 1.18×10^{27} kg (5.93×10^{-4} $M_\odot$) in IRIS, 1.06×10^{28} kg (5.33×10^{-3} $M_\odot$) in AKARI, and 1.06×10^{27} kg (5.33×10^{-4} $M_\odot$) in the WISE survey. We have also studied the visual extinction parameter due to such dust in infrared bands. This work will contribute to understanding infrared band emission from the dusty region around the nebular structure in the interstellar medium.

Keywords: Interstellar medium • Dust color temperature • Dust mass • Visual extinction

I. Introduction

The substance and radiation between stars is known as the interstellar medium (ISM). Nearly 15% of the observable stuff in the Milky Way galaxy is interstellar matter. ISM is mostly composed of hydrogen, with 8.9% of it being helium and 0.1% of heavier components. Ionized hydrogen and cool neutral atomic molecules make up the interstellar gas near hot young stars [1]. The amount of heavy elements in the ISM is gradually rising. The ISM model contains three phases: Molecular hydrogen from the molecular cloud, ionized hydrogen (HII), also known as hot and warm ionized medium, and atomic hydrogen (HI), also known as cold and warm neutral medium (Coronal gas). Planetary nebulae (PN) continue to be of interest due to their importance in studies of

* *Corresponding Author: ajay.jha@cdp.tu.edu.np*

stellar development and their key position in the mass exchange between stars and the interstellar medium (ISM). The planetary nebulae (PN) morphologies range from simple circular to intricate symmetrical designs [2].

A nebula is a large cloud of gas and dust that occurs between stars and serves as the breeding ground for young stars. Dust, fundamental components like hydrogen, and other ionized gases make up nebulae. They can develop as supernova remnants or rigid interstellar gas and dust clouds. The Iris Nebula, commonly known as NGC 7023, is a subject of great interest to astronomers. Reflection Nebulae are illuminated by their exceedingly tiny solid matter particles, which can be up to 10 or even 100 times smaller than the dust on Earth. Due to the light scattering caused by these particles, the nebula has a blue second-hand glow. Although NGC 7023 seems to be primarily blue, it includes enormous strands of deep red, indicating the existence of an unidentified chemical compound likely based on hydrocarbons [3].

Jha and Aryal [4] studied the properties of interstellar dust using the infrared survey in the region near the Pulsars. Poudel et al. [5] performed similar works near the White Dwarfs. Jha & Upadhyay [6], and Gautam et al. [7] studied dusty environments nearby AGB Star and calculated dust temperature. Jha et al. [8] and Poudel et al. [9] studied the dust color temperature of Supernova Remnants . Similar works have been performed by a few researchers nearby Far Infrared (FIR) loops [10], FIR Cavities [11], and Isolated Nebula at different positions in the sky and calculated dust temperature, Planck's function distribution, and dust mass using IRIS and AKARI surveys. In this work, we have studied the dust properties around NGC 7023 Nebula using IRIS, AKARI, and WISE surveys which help to understand the shaping mechanism of ISM and possible physical phenomena are explained.

II. Material and Methods

We have used data from IRIS (60 μm and 100 μm), AKARI (90 μm and 140 μm), and WISE (12 μm and 22 μm) surveys to find flux densities. From SkyView Virtual Observatory (https://skyview.gsfc.nasa.gov/current/cgi/query.pl), FITS images were downloaded for these bands. Aladin v2.5 and v11.0 are used to extract and reduce the data. Each pixel of the FITS image of our region of interest is analyzed by the software Aladin v11.0. We used the Gaia Archive (https://gea.esac.esa.int/archive) for the estimation of the distance of this Nebula.

Dust color temperature

We have used the method of Dupac et al. [12] and Schnee et al. [13] to calculate the dust color temperature.

For IRIS

The expression to calculate the dust color temperature for the IRIS survey is:

$$T_d = \frac{-96}{\ln\left[R \times 0.6^{(3+\beta)}\right]} \tag{1}$$

where flux density ratio, R, is given by:

$$\mathrm{R} = \frac{F(60\ \mu\mathrm{m})}{F(100\ \mu\mathrm{m})} \tag{2}$$

The flux densities at 60 μm and 100 μm, respectively, are F(60 μm) and F(100 μm). The spectral emissivity index value, β, is determined by dust particle parameters such as composition, size, and compaction. For crystalline dielectric, dust has a value of $\beta = 2$ [12].

For AKARI

The expression for dust color temperature in the AKARI survey is:

$$\mathrm{T_d} = \frac{-57}{\ln\left[R \times 0.6^{(3+\beta)}\right]} \tag{3}$$

where flux density ratio, R, is

$$R = \frac{F(90\ \mu\mathrm{m})}{F(140\ \mu\mathrm{m})} \tag{4}$$

Here, $F(90\ \mu\mathrm{m})$ and $F(140\ \mu\mathrm{m})$ are the flux densities at 90 μm and 140 μm respectively.

For WISE

The expression for dust color temperature in the WISE survey is:

$$\mathrm{T_d} = \frac{-546}{\ln\left[R \times 0.54^{(3+\beta)}\right]} \tag{5}$$

where flux density ratio, R, is

$$R = \frac{F(12\ \mu\mathrm{m})}{F(22\ \mu\mathrm{m})} \tag{6}$$

Here, $F(12\ \mu\mathrm{m})$ and $F(22\ \mu\mathrm{m})$ are the flux densities at 22 μm and 22 μm respectively.

Planck's function

Planck's function is given by the equation,

$$\mathrm{B}\left(v,\ \mathrm{T}_d\right) = \frac{2hv^3}{c^2}\left[\frac{1}{e^{\frac{hv}{k_B T}} - 1}\right] \tag{7}$$

where h = Planck's constant, c = velocity of light, ν = frequency at which the emission is observed, and $\mathrm{T_d}$ the average temperature of the region [14].

Dust mass

The dust mass is estimated from the IR flux densities. The resulting dust mass depends on the physical and chemical properties of the dust grains, the adopted dust color temperature ($\mathrm{T_d}$), and the distance (D) [15]. For the calculation of dust mass, first we need the value of flux density ($\mathrm{F_v}$),

$$\mathrm{F}_v = \mathrm{NB}(v, \mathrm{T_d})\mathrm{Q}(v)\mathrm{T_d}\left(\frac{\pi \mathrm{a}^2}{\mathrm{D}^2}\right) \tag{8}$$

where Q(v) is grain emissivity index. The dust mass can be calculated as,

$$M_d = \frac{4\alpha\rho}{3Q(v)}\frac{F(v)D^2}{B\,(v, T_d)} \tag{9}$$

where, α = weighted grain size, ρ = grain density, Q = grain emissivity, F_v = f × MJy/sr × 5.288 $\times 10^{-9}$ where 1MJy/sr = 1×10^{-20} kg s^{-2} and f = relative flux density measured from the image.

Visual Extinction

The empirical formula for the calculation of visual extinction is given by Wood et al. [16],

$$\mathrm{A}v(\mathrm{mag}) = 15.078\left[1 - e^{\frac{-\tau_{100}}{641.3}}\right] \tag{10}$$

Here, τ_{100} = optical depth at 100μm wavelengths, F(100 μm) = flux at 100 μm, And B (v, T_d) = Planck's function at 100 μm.

III. Results and Discussion

Projection map

Fig. 1(a), 1(b), and 1(c) show the IRIS, AKARI, and WISE map projections of NGC 7023, respectively. The candidate is placed in the southern hemisphere on this projection map. The size of the isolated cavity structure in the IRIS is larger than that of the AKARI and WISE, although the resolution of AKARI and WISE is more than IRIS. This difference in the structure size in the projection map is because we have extracted a 50 × 50 size image in IRIS, a 500 × 500 size image in AKARI, and a 150 × 150 size in WISE.

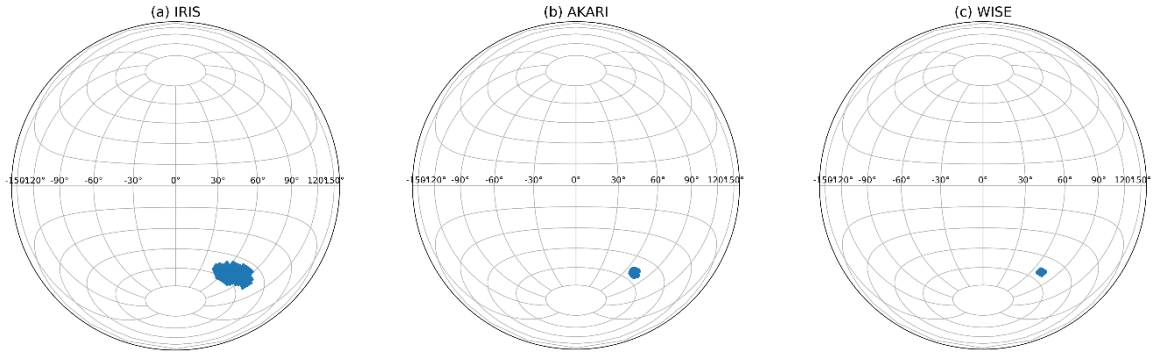

Figure 1. Position of candidate NGC 7023 (a) IRIS, (b) AKARI and (c) WISE.

Linear fit of flux

The flux distributions using a best-fit line between IRIS F60 μm and F100 μm , AKARI F90 μm and F140 μm , and WISE 12 μm and 22 μm along the X and Y axis are shown in Fig. 2 (a), 2(b), and 2(c). From Fig. 2, the flux in the AKARI map is linearly distributed and the slope is found to be 1.67, the intercept is -504.59 MJy/sr , correlation coefficient (r) is 0.87. For IRIS, the flux is more concentrated towards the left side and the slope is 0.79, the correlation coefficient (r) is 0.97. Similarly, for WISE, the slope is 0.08, and the correlation coefficient (r) is 0.97.

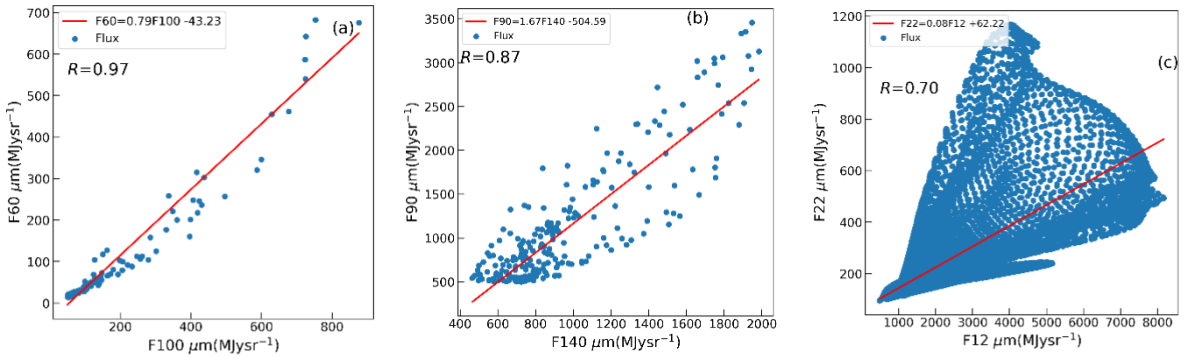

Figure 2. A best-fit line of Flux density with scatter diagram at (a) IRIS F60 μm versus F100 μm , (b) AKARI WIDE-S versus WIDE-L and (c) WISE 22 μm versus 12 μm . The straight line represents the best-fit line, whereas the dots represent the flux.

Distribution of dust color temperature

Fig. 3(a), 3(b), and 3(c) shows the variation of dust color temperature in the IRIS, AKARI, and WISE surveys, respectively. The temperature distribution shows that the core region is hot, and the lower region is cold. In the case of AKARI, maximum and minimum temperatures are 38.80 K $\pm$ 0.25 K, and 21.00 K $\pm$ 0.25 K, respectively. Similarly, for the IRIS, maximum and minimum temperatures are 36.19K $\pm$ 0.03 K and 24.49 K $\pm$ 0.03 K, and the maximum and minimum temperatures for WISE are found to be 130.92 K $\pm$ 0.01 K and 88.71 K $\pm$ 0.01 K respectively. The offset temperature is found to be 17.80 K in AKARI, 11.70 K in IRIS, and 42.21 K in WISE surveys. The minimum temperature region indicates the region has cold ISM matter, and the maximum temperature region indicates the region has warm ISM matter.

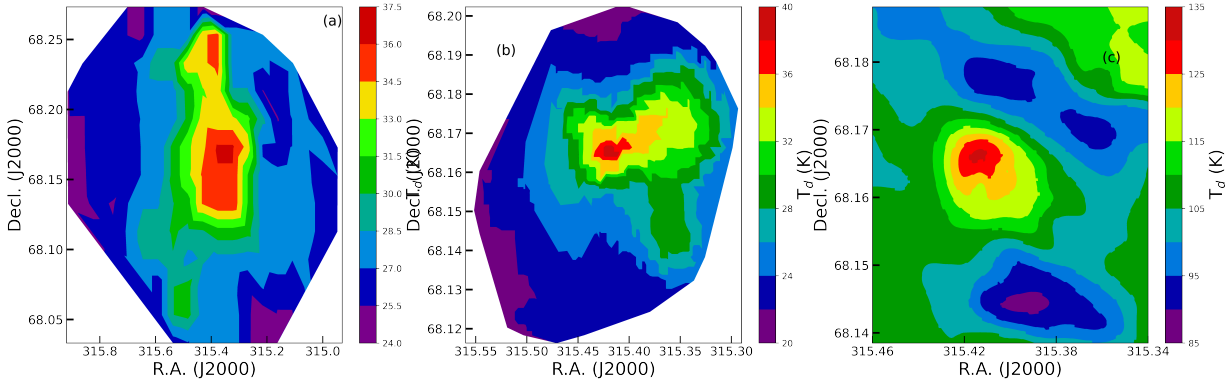

Figure 3. The counter contour plot of (a) Decl. (J2000) versus R.A.(J2000) versus temperature in IRIS (b) Decl. (J2000) versus R.A.(J2000) versus temperature in AKARI and (c) Decl. (J2000) versus R.A.(J2000) versus temperature in WISE at R.A.(J2000) = $21^h\ 01^m35.60^s$, Decl. (J2000) = $+68^o10^m10.0^s$.

Distribution of dust mass

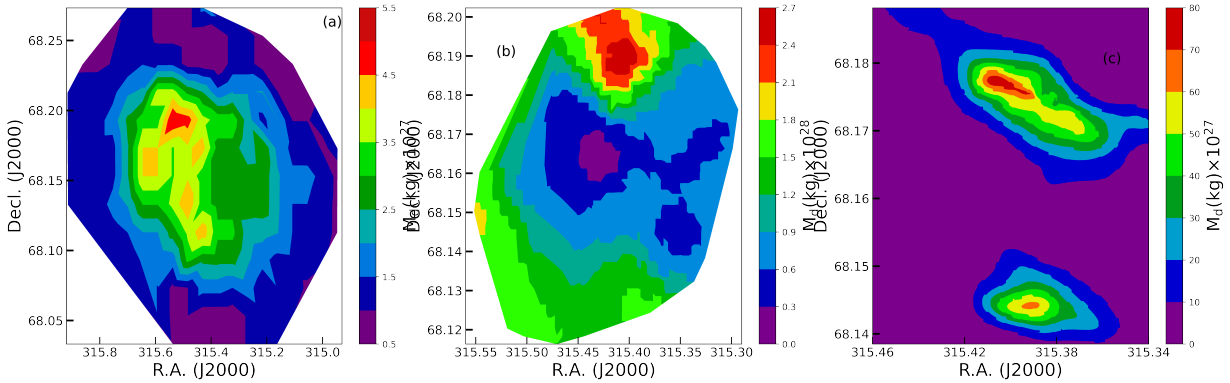

Figure 4. The contour plot of (a) Decl. (J2000) versus R.A.(J2000) versus mass in IRIS, (b) Decl. (J2000) versus R.A.(J2000) versus mass in AKARI and (c) Decl. (J2000) versus R.A.(J2000) versus mass in WISE. The color bar indicates the dust mass distribution (M_d).

Fig. (4(a), 4(b), and 4(c) are the contour plots of the distribution of dust mass in the IRIS, AKARI, and WISE maps. The maximum and minimum dust mass in AKARI is 2.65 × 10^{28} kg and 1.99 × 10^{27} kg, respectively. Similarly, in IRIS, the maximum and minimum dust mass is 3.34 × 10^{27} kg and 4.06 × 10^{26} kg. In WISE, 7.72 × 10^{27} kg is the maximum and 1.06 × 10^{26} kg is the minimum value of dust mass in the nebular region of NGC 7023, respectively.

Distribution of Planck's function

The variations of the Planck function with between R.A. (J2000) and Decl. (J2000) along the horizontal and vertical axis in the contour plot in the IRIS, AKARI, and WISE maps are shown in Fig. 5(a), 5(b), and 5(c). The greater the value of Planck's function in the centre region, the greater the infrared emission in that region

in comparison to the lower regions. From the calculation, it is found that the maximum and minimum values of Planck's function are 1.10 $\times 10^{-14}$ $Wm^{-2}sr^{-1}Hz^{-1}$ and 1.09$\times 10^{-15}$ $Wm^{-2}sr^{-1}Hz^{-1}$ in AKARI, 8.98 $\times 10^{-15}$ $Wm^{-2}sr^{-1}Hz^{-1}$ and 2.21$\times 10^{-15}$ $Wm^{-2}sr^{-1}Hz^{-1}$ in IRIS and 2.54 $\times$ 10^{-13} $Wm^{-2}sr^{-1}Hz^{-1}$ and 2.34 $\times$ 10^{-14} $Wm^{-2}sr^{-1}Hz^{-1}$ in WISE, respectively.

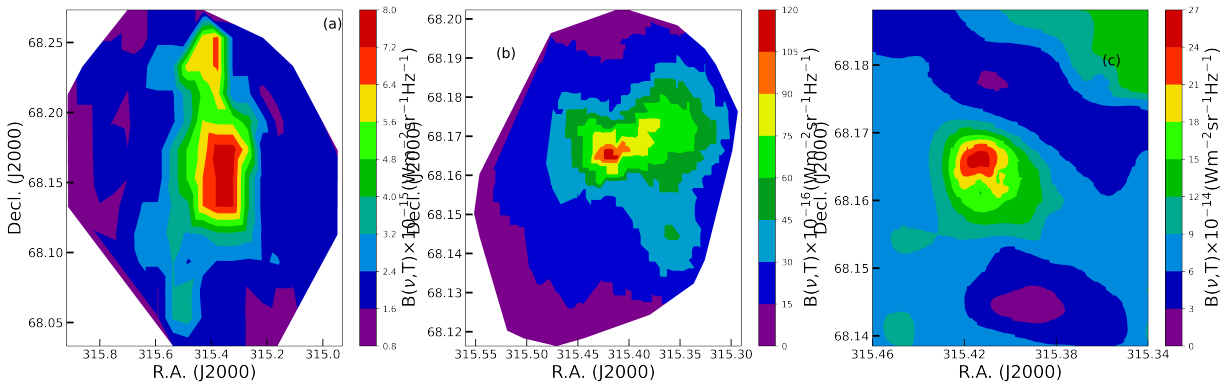

Figure 5. The contour plot of (a) Decl. (J2000) versus R.A.(J2000) versus Planck's function in IRIS (b) Decl. (J2000) versus R.A.(J2000) versus Planck's function in AKARI and (c) Decl. (J2000) versus R.A.(J2000) versus Planck's function in WISE. The color bar indicates the Planck's function distribution B(v, T).

Normal with histogram plot of temperature

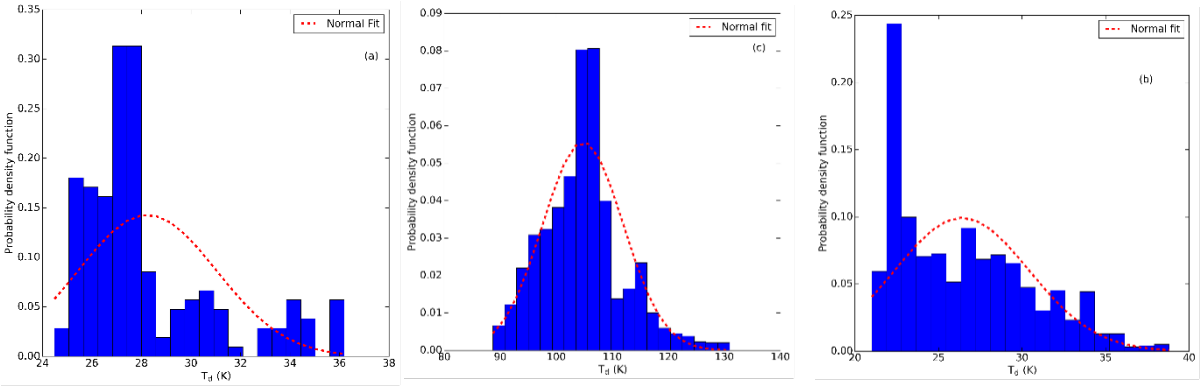

Figure 6. Normal fit with histogram plot of (a) Probability density function versus temperature: IRIS, (b) Probability density function versus temperature AKARI, and (c)Probability density function versus temperature: WISE.

The normal plot with histogram of temperature versus probability density function is shown in Fig. 6 (a), 6(b), and 6(c). The curve is slightly skewed to the right in IRIS and AKARI surveys, and normally distributed in wise survey. The normal center is found to be 27.39 K in IRIS, 25.65 K in AKARI and 104.84 K in WISE.

Normal with histogram plot of dust mass

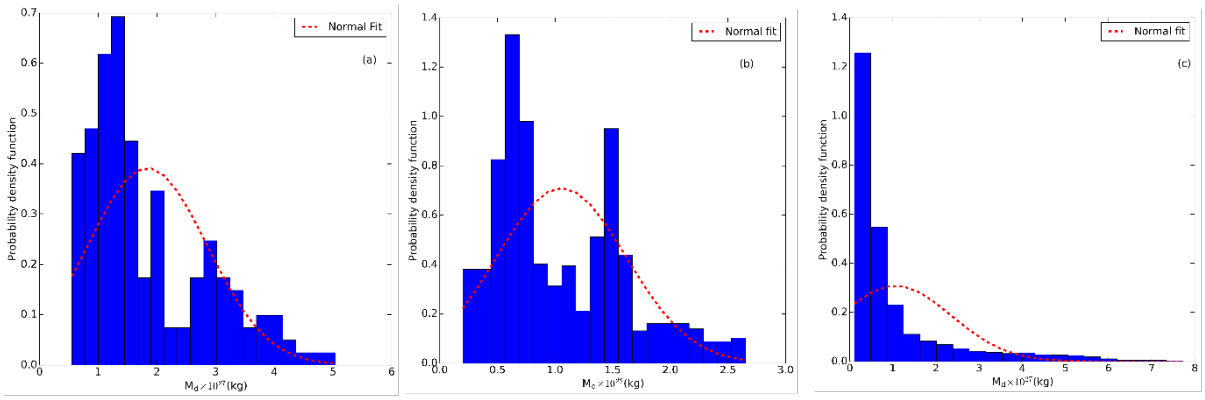

Figure 7. Normal fit with histogram plot of (a) Probability density function versus mass: IRIS, (b) Probability density function versus mass: AKARI and (c) Probability density function versus mass: Wise.

The normal with histogram plot of mass is shown in Fig. 7(a), 7(b), and 7(c). The normal centre is found to be 8.32 × 10^{26} kg in IRIS, 8.69 × 10^{27} kg in AKARI and 5.11 × 10^{26} kg in WISE survey.

Dust color temperature vs visual extinction

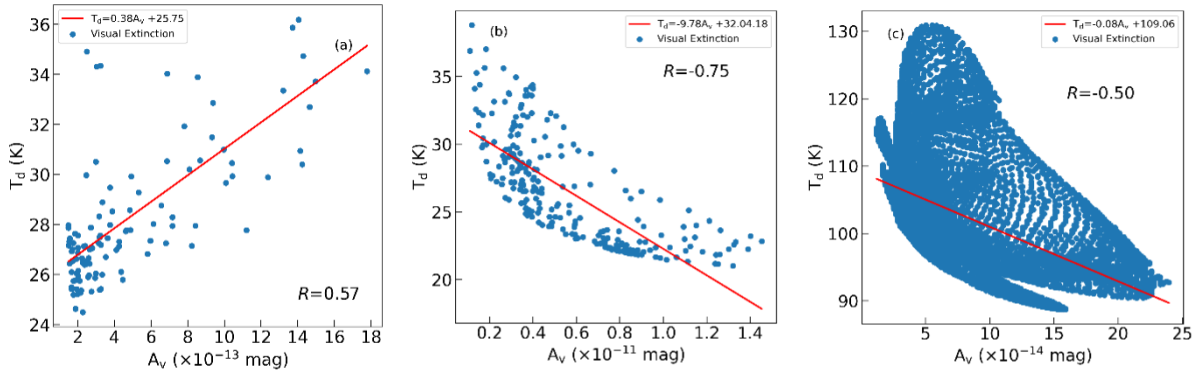

Figure 8. Dust color temperature T_d (K) versus Visual extinction (Av) in the region of interest. (a) IRIS (b) AKARI and (c) WISE surveys.

Fig. 8(a), 8(b), and 8(c) show the variation of visual extinction (A_v) with dust color temperature around the cavity region of NGC 7023 in the IRIS, AKARI, and WISE surveys, respectively. For IRIS, we found the slope value 0.38, intercept = 25.75 (mag), and correlation coefficient = 0.57. This positive value of r indicates a positive correlation between temperature and extinction. For AKARI, we found the slope = -9.78, intercept = 32.04 (mag), and the correlation coefficient = -0.78. Here, the value of r is negative, so there is a negative correlation between (K) and A_v (mag). Similarly, for WISE, we found the slope = -0.81, intercept = 109.06

(mag), and the correlation coefficient = -0.50. This indicates that they are showing the opposite behavior. In AKARI and WISE, we see an inverse relationship between T_d (K) and A_v (mag).

Comparison with previous work

Using the AKARI survey, Gautam et al. [17] investigated the dust color temperature and Planck's function distribution of a far-infrared (FIR) planetary nebula structure at 90 μm and 140 μm . The dust color temperature of the reflection nebula (NGC 7023) is compared to Jha et al. [11] of a far-infrared planetary nebula in the AKARI survey at 90 μm and 140 μm as: from Table 1 it can be seen that the two nebulae have comparable dust color temperature at 90 μm and 140 μm in the AKARI survey.

Table 1. Comparison of dust color temperature in the AKARI survey.

Candidate	Maximum T_d(K)	Minimum T_d (K)	Average T_d (K)	Offset T_d (K)
Planetary Nebula	37.36	16.99	27.18	20
NGC 7023	38.80	21.00	26.39	17.8

Aryal et al. [18] presented a large new high latitude cone-like cloud found at 100 μm and 60 μm IRAS images. They have determined the dust color temperature T_d (K) of the nebula with an average dust color temperature in the region was to be 27 $\pm$ 4 K. in the IRIS survey, we found an average temperature of 28.24 $\pm$ 0.034 K, which is comparatively equal to the previous work.

Table 2. Comparison of dust color temperature in the IRAS survey [19].

Candidate	Average T_d (K)
Cone-like far-IR rebula	27 $\pm$ 4
NGC 7023	28.24 $\pm$ 0.034

IV. Conclusions

We chose NGC 7023, having isolated strong emission structure around the central region for our far-infrared investigation at 60 μm and 100 μm in the IRIS survey, 140 μm and 90 μm in the AKARI survey, and 22 μm and 12 μm in the WISE survey. The dust color temperature, dust mass, and visual extinction are calculated. We found the isolated dust structure interesting and prominent to study in all bands of IRIS, AKARI and WISE. The variance in dust temperature, dust mass, Planck's function, and flux density was determined, and these results were compared and analyzed in IRIS, AKARI, and WISE. We draw the following conclusion from our study:

- The dust color temperature is found in the range between 36.19 K $\pm$ 0.034 K to 24.49 K $\pm$ 0.034 K with an

average dust color temperature 28.24 K ± 0.034 K in IRIS survey and range between 38.80 K ± 0.251 K to 21.00 K ± 0.251 K with an average dust color temperature 26.39 K ± 0.251 K in AKARI survey. Similarly in WISE, the dust color temperature is found in the range between 130.92 K ± 0.009 K to 88.71 K ± 0.009 K with an average 104.76 K ± 0.009 K.

- The dust color temperature was found to be the higher in the WISE survey than that of the IRIS and AKARI survey. Thus, there is inverse relation between the dust color temperature and the wavelength.

- According to the IRIS survey, the maximum and minimum dust mass in our region of interest are 3.34 × 10^{27} kg (1.68 × 10^{-3} $M_{\odot}$) and 4.06 ×10^{26} kg (2.04 × 10^{-4} $M_{\odot}$) respectively. Similarly, 2.65 × 10^{28} kg (1.33 × 10^{-2} $M_{\odot}$) and 1.99 × 10^{27} kg (1.00 × 10^{-3} $M_{\odot}$) in the AKARI survey and 7.72 × 10^{27} kg (3.89 × 10^{-4} $M_{\odot}$) and 1.06 × 10^{26} kg (5.32 × 10^{-5} $M_{\odot}$) in the WISE survey respectively. The dust mass value is higher in AKARI as it has a direct relationship with flux.

- From the contour map, the dust color temperature and dust mass show an inverse relation with each other.

- The visual extinction is found to be in the range of 1.83 × 10^{-12} mag. to 2.23 ×10^{-13} mag. with an average value of 6.46 × 10^{-13} mag. in IRIS, 1.45 × 10^{-11} mag. to 1.09 × 10^{-12} mag. with an average value of 5.78 × 10^{-12} mag. in AKARI and 2.39 × 10^{-13} mag. to 1.17 × 10^{-14} mag. With an average value of 5.31 × 10^{-14} mag. in WISE. This result shows the inverse relationship between extinction and temperature. This supports the fact that the higher the temperature, the lower will be the visual extinction.

V. Acknowledgements

We appreciate the referee's helpful feedback and insightful remarks. We would like to acknowledge Aladin, Skyview virtual observatory, SIMBAD, IRAS, AKARI, and WISE surveys. Two authors (AKJ & SNY) acknowledge UGC, Nepal, for providing a faculty research grant no.FRG-075/076-S&T-2.

References

[1] Ferriere KM. The interstellar environment of our galaxy. Reviews of Modern Physics. 2001;73(4):1031.

[2] Borkowski KJ, Sarazin CL, Soker N. Interaction of planetary nebulae with the interstellar medium. The Astrophysical Journal. 1990;360:173-83.

[3] Boutéraon T, Habart E, Ysard N, Jones A, Dartois E, Pino T. Carbonaceous nano-dust emission in protoplanetary discs: the aliphatic-aromatic components. Astronomy & Astrophysics. 2019;623:A135.

[4] Jha A, Aryal B. A study of a cavity nearby a pulsar at-60^{o} latitude in the far infrared map. Journal of Nepal Physical Society. 2017;4(1):33-41.

[5] Paudel M, Bhandari P, Bhattarai S. Study of dust cavity around the white dwarf wd 0352-049 in infrared astronomical satellite map. Journal of Nepal Physical Society. 2021;7(2):110-8.

[6] Jha A, Upadhyay D. Dust Structure around two Asymptotic Giant Stars at Latitude 32 & 40.67. Himalayan Physics. 2017:41-7.

[7] Gautam SP, Silwal A, Tiwari M, Subedi S, Khanal M, Jha AK. Dust Properties of Two New Cavity Structures Nearby Asymptotic Giant Branch Stars: The IRAS Survey. Journal of Institute of Science and Technology. 2021;26(2):119-26.

[8] Jha A, Yadav A, Upadhyay D, Aryal B. Dust Properties of Super-Nova Remnant (Crab Nebula) Using AKARI Survey. Journal of Nepal Physical Society. 2021;7(4):64-70.

[9] Paudel M, Bhattarai S. Studies of the Properties of Dust Structure Nearby the Supernova Remnants G053. 41+ 00.3, G053. 9+ 00.2 and G053. 1+ 00.3 using Data from IRIS and AKARI. Journal of Nepal Physical Society. 2021;7(3):59-66.

[10] Jha A, Aryal B, Weinberger R. A study of dust color temperature and dust mass distributions of four far infrared loops. Revista mexicana de astronomía y astrofísica. 2017;53(2).

[11] Jha A, Aryal B. Dust color temperature distribution of two FIR cavities at IRIS and AKARI maps. Journal of Astrophysics and Astronomy. 2018;39:1-7.

[12] Dupac X, Bernard JP, Boudet N, Giard M, Lamarre JM, Mény C, et al. Inverse temperature dependence of the dust submillimeter spectral index. Astronomy & Astrophysics. 2003;404(1):L11-5.

[13] Schnee SL, Ridge NA, Goodman AA, Li JG. A complete look at the use of IRAS emission maps to estimate extinction and dust temperature. The Astrophysical Journal. 2005;634(1):442.

[14] Tiwari M, Gautam S, Silwal A, Subedi S, Paudel A, Jha A. Study of Dust Properties of two Far Infrared Cavities near by Asymptotic Giant Branch stars under Infrared Astronomical Satellite Maps. Himalayan Physics. 2020:60-71.

[15] Hildebrand RH. The determination of cloud masses and dust characteristics from submillimetre thermal emission; 1983.

[16] Wood DO, Myers PC, Daugherty DA. IRAS images of nearby dark clouds. The Astrophysical Journal Supplement Series. 1994;95:457-501.

[17] Gautam S, Silwal A, Jha A. Dust color temperature and Planck function distribution of a far infrared planetary nebula at 90 and 140 μm AKARI map. International Astronomy and Astrophysics Research Journal. 2020:1-8.

[18] Aryal B, Weinberger R. A new large high latitude cone-like far-IR nebula. Astronomy & Astrophysics. 2006;448(1):213-9.